

Synthesis of Nickel Selenide Nanoparticles as Cathode Material for Zink Ion Batteries and Study of Their Optical Properties

Jaiveer Singh^{1,a}, Jitendra Tripathi^{1,b}, Puja Singh^{2,c} and Mayank Sharma¹

¹Department of Physics, ISR, IPS Academy, Indore, M.P., India.

²Department of Electronics & Communication Engineering, Medi-Caps University, Indore, M.P., India.

^a jaiveer24singh@gmail.com

^b jtripathi00@gmail.com

^c puja.singh@medicaps.ac.in

Abstract

Porosity of electrode materials has been proven to be very significant in enhancing the performance of Zn-ion batteries (ZIB) in recent studies. On a positive electrode, porosity improves its kinetics by faster electron transport and richer electro active reaction sites. On a negative electrode, porous structure provides increased surface area and reduced local current density, both favorable to the performance of ZIB. Nickel Selenide (NiSe) nanoparticles (NPs) can be considered as more suitable cathode materials also due to their smaller band gap and higher conductivity. We have synthesized NiSe nanoparticles using a chemical method with octylamine as a surfactant with crystallite size of 36 nm. The field emission scanning electron microscopy (FESEM) images shows the formation of spikelike structure making the nanoparticles highly porous making them even more suitable as a cathode material.

Keywords: Nanoparticles, X-Ray Diffraction (XRD), FESEM.

Received 28 January 2025; First Review 11 February 2025; Accepted 27 April 2025.

* Address of correspondence

Jaiveer Singh
Department of Physics, ISR, IPS Academy,
Indore, M.P., India.

Email: jaiveer24singh@gmail.com

How to cite this article

Jaiveer Singh, Jitendra Tripathi, Puja Singh and Mayank Sharma, Synthesis of Nickel Selenide Nanoparticles as Cathode Material for Zink Ion Batteries and Study of Their Optical Properties, J. Cond. Matt. 2025; 03 (02): 137-140.

Available from:
<https://doi.org/10.61343/jcm.v3i02.80>



Introduction

Transition Metal Selenides (TMS) have been a subject of interest in the field of nanotechnology recently due to spectrum of properties ranging from insulators to semiconductors and semiconductors to true metals [1,2]. Transition metals are known to make variety of complexes due to their d-block electronic configuration and Nickel is no exception in that regard. In addition, due to small difference in the electronegativity of nickel and selenium they make several different phases of nickel selenides (i.e., NiSe, NiSe₂, Ni₃Se₂, and Ni₃Se₄) with different physical and chemical properties [3,4]. The band gap of NiSe falls between the conductor and semiconductors which makes it a very suitable candidate for the cathode material in Zn ion Batteries (ZIB) [5,6].

Another factor that significantly affects the performance of cathode material is their capacity to accommodate the Zn⁺. This is where the porosity of the cathode materials plays an important role. A sufficiently porous cathode material can accommodate the Zn⁺ ion easily which will allow the chemical reaction to take place with ease and also porosity

will significantly increase the surface area available for the chemical reactions.

The phase as well as the size, shape and morphology of the NPs have always been dependent on the synthesis techniques used and various reaction parameters. There are so many physical and chemical methods have been used for the synthesis of metallic nanoparticles. But among of them Chemical method is one of the most convenient and commonly used techniques to synthesize nanoparticles. Due to its low temperature threshold and low-cost ingredients in which precursors are mixed at an elevated temperature (near 200 °C) in an organic solvent which also acts as the surfactant [2-5]. Herein, we have optimized a much simpler method to synthesize single phased nickel selenide NPs with the use of a single surfactant. With this method, we were able to synthesize highly porous nanoparticles of NiSe. The purity and structural properties of the sample was studied with the help of different characterization techniques. The FESEM images clearly show the formation of spike-like structures creating the micropores throughout the sample. The low intensity peaks in powder X-ray diffraction spectroscopy (XRD) further support the

formation of micropores.

Experiment

General

All chemicals such Nickel chloride hexahydrate ($\text{NiCl}_2 \cdot 6\text{H}_2\text{O}$) with purity $\geq 98\%$ and selenium (Se) powder with purity 99.99% trace metals basis of standard grade were used. Octylamine with purity 99% was used as solvent or reducing material. Octylamine is selected because it has strong solubility in organic systems, mild reactivity, and the capacity to increase dispersion, guide particle development, and give surface passivation. All chemical were purchased from Sigma Aldrich. Ethanol was purchased from Changshu Hongsheng Fine Chemical Co. Ltd

Synthesis

Nickel selenide (NiSe) nanoparticles were synthesized via a bottom-up chemical approach. In this typical procedure, Nickel chloride hexahydrate ($\text{NiCl}_2 \cdot 6\text{H}_2\text{O}$) and selenium (Se) powder were used as precursors in a 1:1 molar ratio of (Ni/Se – 1:1). These precursors were mixed with 6 mL of octylamine in a 50 mL round-bottom flask. The flask was then sealed and heated at 18°C for 2h. After the completion of the reaction, the mixture was allowed to cool up to the room temperature (25°C). A black precipitate was obtained and indicating the successful formation of NiSe nanoparticles. The product was washed by adding 20 ml of ethanol 4 times to remove the excess amount of octylamine and other byproducts. After washing the resulting NPs sample was dried in oven at 60°C for 6 hours and ground very well. The NiSe NPs powder was moved to a vacuum-sealed vial and kept in a glove box following synthesis. As a result, the material's integrity was maintained with little exposure to oxygen and moisture. Additionally, characterizations were performed using the produced NPs sample.

Characterizations

The XRD measurement of the sample was done by Bruker D8 Advance- Powder XRD with $\text{CuK}\alpha$ radiation ($\lambda = 1.5406 \text{ \AA}$) to examine the purity, phase and crystallinity of the sample. The 2θ range was selected from 20° to 90° with step size of 0.02. The morphology of the nanoparticles was studied using FE-SEM in energy range of 20 keV. UV-vis spectroscopy was performed by Shimadzu UV-VIS spectrophotometer Model: UV-1800 was used to analyse the optical properties and band gap of the synthesized NPs.

Results and Discussion

Structural property of the NiSe NPs were determined by XRD measurement. The XRD Pattern of NiSe shown in Figure 1.

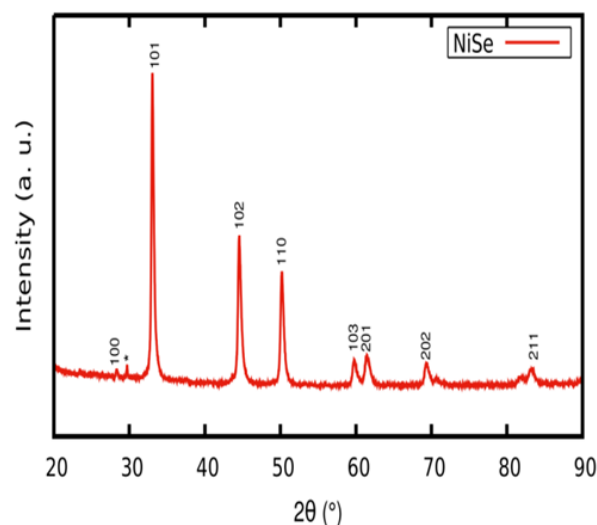


Figure 1: XRD pattern of Hexagonal NiSe sample. The bragg's planes are indicated by their miller indices. The small peaks marked by (*) are due to pure selenium remained in the sample.

Which shows the presence of single phased hexagonal Nickel Selenide crystals (PC-PDF No. - 89-7160) belonging to the space group P-63/mmc (194). The diffraction peaks corresponding to the planes (100), (101), (102), (110), (103), (201), (202) and (211) at 2θ values 28.1, 33.15, 44.69, 50.33, 59.9, 61.7, 69.6 and 83.5° respectively. The highest peak was observed for the plane (101).

The crystallite size was calculated using Dabey-Scherrer method by taking the most intense peak (101) for the calculation using the Debye Scherrer formula. Where D - Crystallite size, K -Scherrer constant ($K = 0.9$) λ - X-ray wave- length ($\lambda = 1.5406 \text{ \AA}$), β - Full width at half maxima (FWHM) and θ is the Braggs' diffraction angle [6].

$$D = \frac{k\lambda}{\beta \cos \theta} \quad (1)$$

Scherrer formula gives information about the crystallite size based on the peak broadening. The crystallite size was determined to be 36 nm. And dislocation density (δ) is found to be $0.01 (\text{nm})^{-2}$. A small dislocation density measurement suggests that there was a significant degree of crystallinity in the generated NiSe nanoparticles. The strain (ϵ) value of NiSe nanoparticles is found 1.5×10^{-4} by Williamson Hall plot which is not included here. This result also shows that the nanoparticle product is a lack of strain.

The lattice parameters 'a' and 'c' for hexagonal Nickel Selenide NPs samples were obtained considering all lattice planes by using following formulas:

$$d_{hkl} = \frac{(h^2 + k^2 + hk)}{3a^2} + \frac{l^2}{c^2} = \frac{\lambda^2}{4\sin^2 \theta} \quad (2)$$

Where d is the inter-planer spacing and (hkl) are miller indices. After calculating the lattice parameters corresponding to different lattice planes, precise lattice parameters were obtained using Nelson-Riley Function given by the relation-

$$F(\theta) = \frac{\cos^2 \theta}{\sin \theta} + \frac{\cos^2 \theta}{\theta} \quad (3)$$

In this approximation method the lattice parameter obtained for different Bragg's angle (corresponding to different planes) are plotted against the $F(\theta)$ and linear regression is used to calculate y-intercept, by extrapolating the straight line to $F(\theta) = 0$ [6]. The obtained values are $a = 3.5222 \text{ \AA}$ and $c = 5.1546 \text{ \AA}$ which are also in good agreement with the standard values of 'a' and 'c' of Nickel Selenide crystals.

FESEM Analysis

In further study, as prepared NiSe NPs sample was characterized for its morphology by FESEM. The results have been shown in FESEM micrograph Figure 2(a, b) at different resolution.

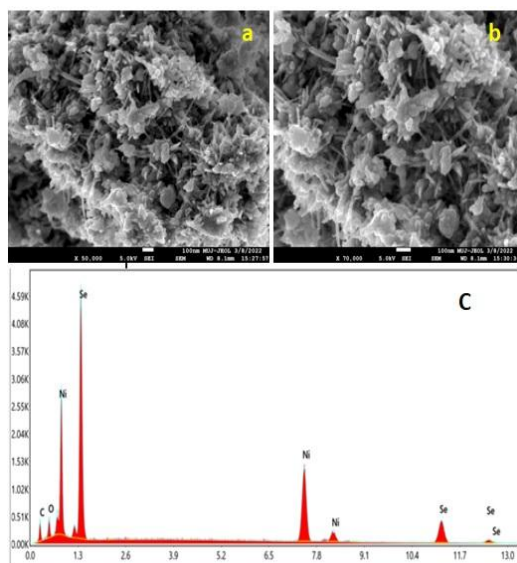


Figure 2: (a, b) FE-SEM and (c) EDX images of NiSe NPs.

It was observed that spikes like structures of size between the range of 20-30nm formed. These spikes cause the formation of random inter-particle micropores of size varying between a few nanometres to micrometers. The elemental components of the nanoparticle specimens produced by chemical method were identified using EDX spectroscopy. Figure 2c shows the range of findings for the NiSe nanoparticles up to a calcination temperature of 500 °C. The Ni and Se elements in the sample are indicated by the pertinent peaks along with weak oxygen peak which may have originated from the molecules that are bound to the surface of NiSe NPs. Consequently, EDX data verified that a chemical method was successfully used to

manufacture pure NiSe nanoparticles. The EDX pattern (Fig. 2c) confirms the presence of Ni and Se in sample.

UV-Vis Spectroscopy

UV- Visible spectroscopy measurement was done in the wavelength range 200-900 nm. The UV-vis absorbance spectrum of the sample was obtained from Defused Reflectance Spectroscopy (DRS). Fig. 3 shows the graph between absorbance and wavelength. UV-visible spectroscopy provides a non-destructive method for examining a nanomaterial's optical properties. In order to analyze scattered and absorbed light from an inhomogeneous NiSe nano powder, the Kubelka-Munk (K-M) relation (Eq. 4) may be used efficiently. Although there is absorption of light by the sample throughout the spectrum but there is a significant drop at about 340 nm of wavelength. Tau's c plot was plotted inside the fig.3 using the relation in Eq. 5 ($\gamma = 2$) [7-9].

$$F(R_{\infty}) = \frac{(1-R_{\infty})^2}{R_{\infty}^2} \quad (4)$$

$$(F(R_{\infty}) \cdot h\nu)^{\frac{1}{\gamma}} = B(h\nu - E_g) \quad (5)$$

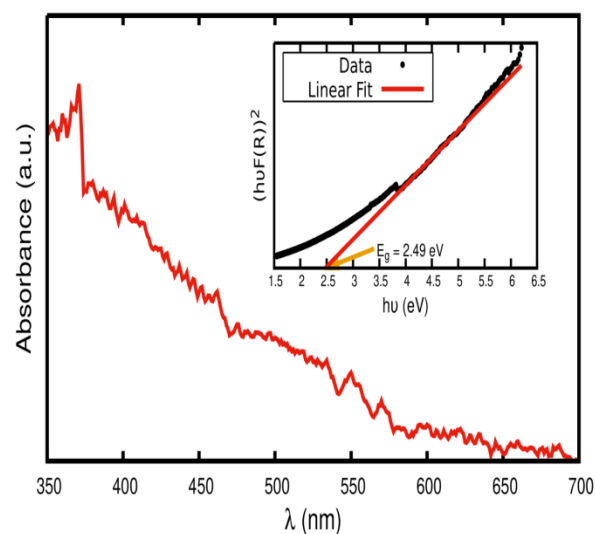


Figure 3: UV-vis absorbance spectrum and in inset Tauc plot for the NiSe NPs.

The band gap of 2.49 eV from a Tauc plot was observed. Which is found in the range of semiconductors with higher conductivity than the conventional electrode such as graphite. While band gap of bulk nickel selenide (NiSe) typically falls in the range of 0.2 to 1.0 eV. It was observed that there is a significant change in band gap from bulk to NPs this is due to the quantum size effect. Here, the quantum size effects become active when the size of NiSe approaches or falls below the exciton Bohr radius. As a result, energy levels become discretized, and electrons and holes are confined in a tiny area. Therefore, the band gap increases as more energy is needed to drive an electron from

the valence band to the conduction band.

Electrochemical Analysis

Nickel selenide (NiSe) stands out among zinc-ion battery (ZIB) cathodes due to its high electronic conductivity and decent structural stability, making it a promising alternative to more traditional oxide-based cathodes. Although, we did not perform electrochemical tests but on the basis of literature, we observed that NiSe is found attractive due to its high electronic conductivity, multiple oxidation states of Ni and layered crystal structure. Compared to manganese dioxide (MnO₂), which offers higher specific capacities (up to 300 mAh/g), NiSe typically delivers moderate capacities in the range of 150–250 mAh/g. However, MnO₂ suffers from poor cycling stability due to structural degradation and manganese dissolution, whereas NiSe maintains better stability over extended cycling. Vanadium-based cathodes like V₂O₅ can provide even higher capacities (300–400 mAh/g), but often face issues with phase transitions and relatively lower conductivity, necessitating conductive additives or structural engineering. Overall, while NiSe may not top the chart in terms of capacity, its superior conductivity, moderate voltage range, and promising stability make it a balanced and practical candidate for next-generation aqueous ZIB cathodes [10].

Conclusion and Future Prospective

In summary, we have successfully synthesized a single phase NiSe nanoparticle which show inter particle microporous structures which has been considered significantly useful in enhancing the performance of ZIB by providing better accommodation capacity for Zn²⁺ ions. The relatively low intensity peaks of XRD also support the same. The band gap obtained from the UV-Vis Spectroscopy confirms the suitable electrical conductivity of the sample for the propose of electrode materials as well. For the precise measurement of the degree and size of porosity as well as the effect of reaction parameter on the porosity of the nanoparticles, further experimentation will be conducted in our future studies.

References

1. N Abbas, J-M. Zhang, S Nazir, M T Ahsan, S Saleem, U Ali, N Akhtar, M Ikram, R Liaqat, A comparative study of structural, vibrational mode, optical and electrical properties of pure nickel selenide (NiSe) and Ce-doped NiSe nanoparticles for electronic device applications, *Phys. B Condens. Matter*, Volume 649, 414471, 2023. <https://doi.org/10.1016/j.physb.2022.414471>
2. C T Lu, S Dong, C Zhang, L Zhang, and G Cui, *Fabrication of transition metal selenides and their applications in energy storage*, *Coord. Chem. Rev.*, 332:75-99, 2017. <https://doi.org/10.1016/j.ccr.2016.11.005>
3. N Moloto, M J Moloto, N J Coville, and S S Ray, *Optical and structural characterization of nickel selenide nanoparticles synthesized by simple methods*, *J. Cryst. Growth*, 311: 3924–3932, 2009. <https://doi.org/10.1016/j.jcrysgro.2009.06.006>
4. Z Zhuang, Q Peng, J Zhuang, X Wang, and Y Li, *Controlled Hydrothermal Synthesis and Structural Characterization of a Nickel Selenide Series*, *Chem. Eur. J.*, 12: 211 – 217, 2006. <https://doi.org/10.1002/chem.200500724>
5. B Yuan, W Luan and S Tu, *One-step solvothermal synthesis of nickel selenide series: Composition and morphology control*, *Cryst. Eng. Comm.*, 14:2145–2151, 2012. <https://doi.org/10.1039/C2CE06474J>
6. P Kumara, S Pathak, A Singh, H Khanduri, Kuldeep, K Jain, J Tawale, L Wang, G A Basheed, R P Pant, *Enhanced static and dynamic magnetic properties of PEG-400 coated CoFe₂-xEr_xO₄ (0.7 ≤ x ≤ 0) nano ferrites*, *Journal of Alloys and Compounds*, 887:161418, 2021. <https://doi.org/10.1016/j.jallcom.2021.161418>
7. S Altaf, H Ajaz, M Imran, A Ul-Hamid, M Naz, M Aqeel, A Shahzadi, A Shahbaz, M Ikram, *Synthesis and characterization of binary selenides of transition metals to investigate its photocatalytic, antimicrobial and anticancer efficacy*, *Appl. Nanosci.*, 10: 2113–2127, 2020. <https://doi.org/10.1007/s13204-020-01350-w>
8. J K Cooper, A M Franco, S Gul, C Corrado and J Z Zhang, *Characterization of Primary Amine Capped CdSe, ZnSe, and ZnS Quantum Dots by FT-IR: Determination of Surface Bonding Interaction and Identification of Selective Desorption*, *Langmuir*, 27 (13): 8486-8493, 2011. <https://doi.org/10.1021/la201273x>
9. P Makuła, M Pacia, and Wojciech Macyk, *The J. Phys. Chem. Lett.*, 9 (23): 6814-6817, 2018. <https://doi.org/10.1021/acs.jpcllett.8b02892>
10. Y Zhang, C Wu, G Liang et al, *Recent Advances in Transition Metal Selenide Cathodes for Aqueous Zinc-Ion Batteries*, *Adv. Funct. Mater.*, 30(42), 2004690, 2020. <https://doi.org/10.1002/adfm.202004690>